VERSF – TPB Overlap as a Phase-Coherent Geometry

A Structural Mechanism for Flat Rotation Curves from Entropy-Driven Coherence

Keith Taylor VERSF Theoretical Physics Program

Table of Contents

Abstract (General Reader)

One of the deepest puzzles in modern physics is that galaxies don't behave the way gravity predicts. Stars at the edges of spiral galaxies orbit at roughly the same velocity as stars near the centre — but if gravity only comes from the matter we can see (stars, gas, dust), those outer stars should be flying off into space. The standard explanation is "dark matter": an invisible substance, never directly detected, that forms a vast halo around each galaxy and provides the extra gravitational pull needed to hold everything together.

This paper proposes a different explanation rooted in the VERSF (Void Energy-Regulated Space Framework) and its Ticks-Per-Bit (TPB) model. In VERSF, when matter undergoes irreversible change — a quantum state committing to one outcome — it produces a "bit": a permanent addition to the universe's informational record. These commitments are what constitute time. Crucially, the structural consequences of each commitment are not confined to the matter that produced it; they spread locally outward through the surrounding quantum foam, altering the distinguishability structure of nearby space.

In a disk galaxy, billions of stars and gas clouds all produce bits and project their influence outward. Because the sources are arranged in a thin disk, these projections overlap most densely in the galactic midplane, forming a thin band of enhanced informational structure. This band is effectively two-dimensional — and in two dimensions, gravitational-like forces fall off as $1/R$ rather than the $1/R^2$ of ordinary three-dimensional gravity. A $1/R$ force is precisely what is needed to produce flat rotation curves — the signature phenomenon attributed to dark matter.

In short: what we interpret as dark matter may be the geometric fingerprint of overlapping bit projections in disk galaxies — not an invisible substance, but an emergent property of how matter's irreversible commitments reshape the structure of surrounding space.

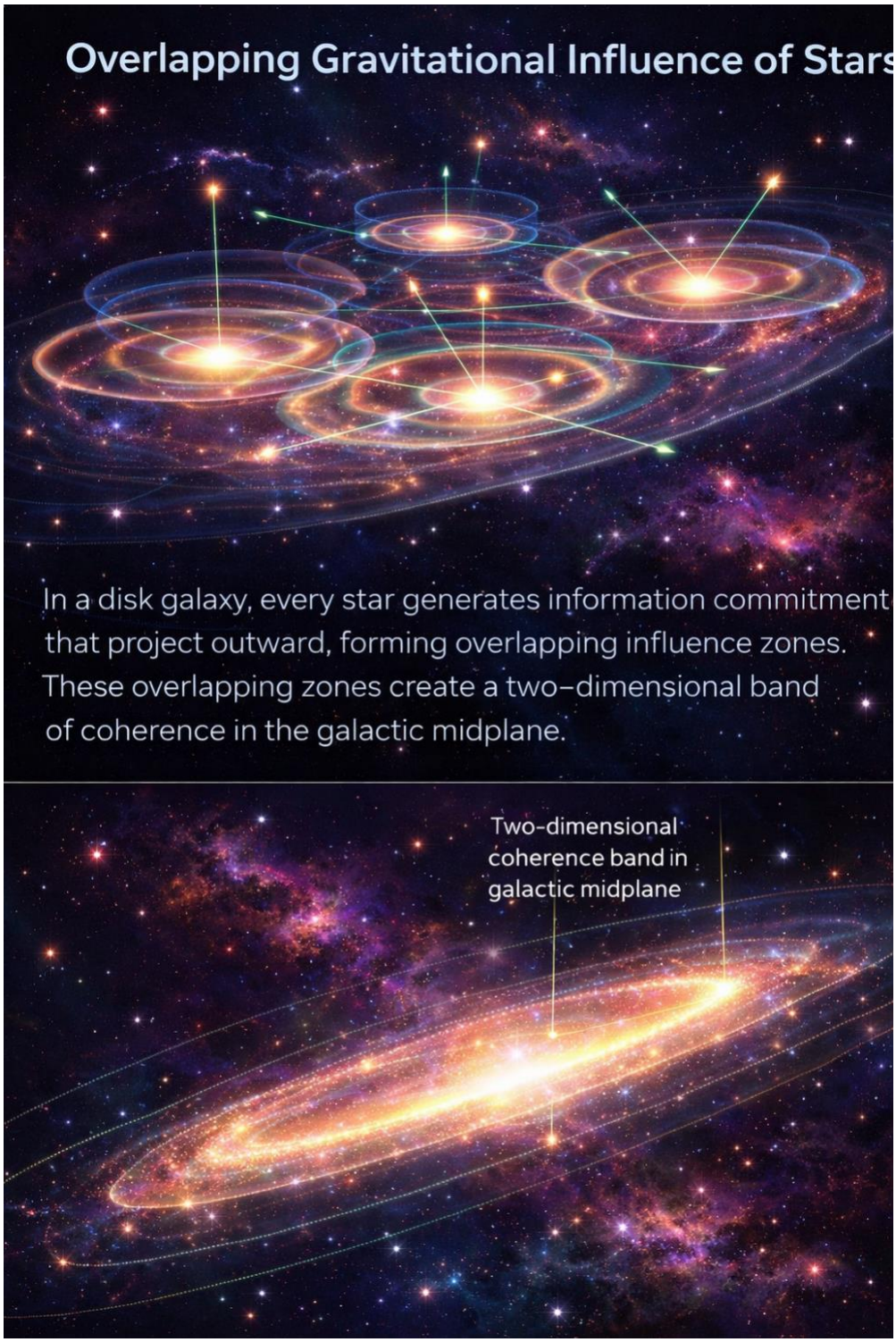

Abstract (Technical)

We show that the galactic rotation curve anomaly — conventionally attributed to dark matter halos — can arise as a structural consequence of phase-coherent overlap in the Ticks-Per-Bit (TPB) framework within VERSF. In TPB, irreversible informational commitments by baryonic matter project distinguishability structure into the surrounding substrate; in disk galaxies, geometric superposition concentrates this structure into a thin midplane band. Beginning from a three-dimensional Landau–Ginzburg energy functional for a TPB overlap order parameter with a spatially varying commitment-driven ordering control parameter a(**x**), we derive (rather than assume) the confinement of the massless phase mode to a thin coherence band Σ coinciding with the galactic disk. The dimensional reduction to a two-dimensional phase theory on Σ follows from the vanishing of phase stiffness outside the ordered region. The resulting 2D Poisson equation for the phase field possesses a logarithmic Green's function, yielding 1/R acceleration profiles and flat rotation curves over the coherence band. A screening mass from finite coherence length provides a natural outer cutoff. We map the effective potential back into the language of local Newtonian gravity and recover a $\rho_{eff} \propto 1/R^2$ profile — the isothermal halo. The mechanism is specific to geometries supporting thin ordered bands (disk galaxies); this regime-specificity is noted and discussed. No new particles are introduced. Throughout, we use natural units ($c = \hbar = 1$) unless otherwise stated, and a $(-,+,+,+)$ metric signature.

---

1. The Rotation Curve Problem in Local Geometric Gravity

For the general reader: Einstein's General Relativity tells us that matter curves spacetime, and that curvature is what we experience as gravity. For a galaxy, once you move beyond the visible matter, you're in "empty" spacetime — and the theory predicts that gravity should weaken as $1/R^2$, just like for the solar system. But galaxy rotation curves show gravity weakening only as $1/R$ out to enormous distances. Something is missing from the standard picture.

1.1 The Vacuum Exterior Problem

In General Relativity, the Einstein field equations relate spacetime curvature to the distribution of matter and energy:

$$G_{\mu\nu} = 8\pi G\, T_{\mu\nu} \quad (1)$$

where $G_{\mu\nu}$ is the Einstein tensor encoding curvature and $T_{\mu\nu}$ is the stress-energy tensor encoding matter content. In the weak-field limit with $g_{00} \approx -(1 + 2\Phi)$, the field equations reduce to a Poisson equation for the Newtonian potential Φ:

$$\nabla^2\Phi = 4\pi G\, \rho \quad (2)$$

Outside a compact baryonic distribution (where $\rho = 0$), this becomes the vacuum Laplace equation:

$\nabla^2\Phi = 0$ (3)

For a spherically symmetric mass distribution, the unique exterior solution is the familiar Newtonian potential:

$\Phi(r) = -GM/r$, $a(r) = GM/r^2$ (4)

where $a(r) = |\partial_r\Phi|$ is the gravitational acceleration.

1.2 Why Flat Rotation Curves Cannot Arise from Vacuum Geometry

Flat rotation curves require $v(r) \approx v_\infty$ = constant at large radii. For circular orbits, the centripetal condition $v^2/r = a(r)$ gives:

$a(r) = v_\infty^2/r \propto 1/r$ (5)

This 1/r scaling is incompatible with the $1/r^2$ acceleration from Eq. (4). More precisely: no solution to the three-dimensional vacuum Laplace equation (3) produces a potential with $\partial_r\Phi \propto 1/r$ at large r. The logarithmic potential $\Phi \propto \ln r$ that would yield this acceleration is a solution to the *two-dimensional* Laplace equation, not the three-dimensional one.

Therefore, within strictly local geometric gravity, matching observed rotation curves requires either:

- **(a)** an additional, unseen source of stress-energy (dark matter), or
- **(b)** a mechanism that introduces an effectively two-dimensional gravitational structure.

This paper develops option (b) within the VERSF–TPB framework.

---

2. Time, Bits, and Overlap: The Physical Picture

This section is written for the general reader and contains no equations. Readers familiar with the VERSF–TPB framework may skip to Section 3.

2.1 Time Is Made of Commitments

We are accustomed to thinking of time as a river — something that flows whether or not anything is in it. VERSF proposes something different: time does not flow on its own. It is produced, and only by specific kinds of events.

When matter — a star, a gas cloud, a particle — undergoes an irreversible change, information that was uncertain becomes definite. A quantum state that could have gone several ways commits to one outcome. That commitment is a bit: a permanent, irreversible addition to the

universe's informational record. It cannot be taken back. And it is these irreversible commitments, accumulating one after another, that constitute what we experience as the passage of time.

Where there is mass, there are bits being produced. Where there is no mass, there are no irreversible commitments — and time, in the VERSF sense, does not advance. Vacuum fluctuations in the quantum foam are reversible and do not produce lasting informational commitments; they do not generate bits and therefore do not constitute time advancement in the TPB sense.

2.2 Bits Don't Stay Put

A crucial feature of bit production is that its effects are not confined to the location where mass sits. When a star generates irreversible commitments, the structural consequences of those commitments alter the distinguishability structure of the surrounding space, and this alteration spreads locally from site to site through the foam — much like a television screen projecting an image beyond its own surface. The bit activity at the source reaches into the space around it, carrying distinguishability and informational structure outward.

Every massive object in a galaxy does this. Every star, every gas cloud, every dense concentration of matter produces bits and locally reshapes the informational structure of its surroundings.

2.3 The Quantum Foam: Stage, Not Actor

If bit projections propagate outward, what are they propagating through?

The answer is the quantum foam — the seething, fluctuating microstructure of space itself. The foam is rich with reversible micro-fluctuations: activity that explores possibilities but never commits to outcomes. Nothing irreversible happens in the foam on its own. It does not produce bits. It does not advance time. It is, in the language of VERSF, temporally sterile.

But this does not mean the foam is unimportant. It is the medium through which bit projections travel. It defines what "nearby" means. It determines the local rules by which projections spread, combine, and decay. Just as air is passive with respect to sound — it does not create sound waves, but it determines how they propagate, interfere, and decay — the quantum foam is passive with respect to bit projections, but it shapes everything about how they behave.

2.4 Overlap: Where Projections Superimpose

Now consider a disk galaxy: a vast, flattened collection of hundreds of billions of stars and gas clouds, all producing bits, all projecting their influence outward through the foam.

Imagine each source as a screen projecting its image into the surrounding space. In a random scatter of sources, those projections spread in all directions and thin out quickly. But in a disk, something geometrically special happens: because the sources are concentrated in a thin plane,

every point near the midplane receives overlapping projections from many nearby sources simultaneously. The midplane of the disk becomes the zone where the greatest number of projections superimpose. This does not require signals to converge from afar; it follows from the local spreading of projection influence from many nearby sources whose geometry is already disk-shaped.

This superposition is the overlap. Where projections from many sources pile up in the same region, the effective information density — the density of bit influence — increases beyond what any single source contributes. The foam does not amplify this effect; it simply allows it to occur. The enhancement is purely geometric: it is the shape of the disk that concentrates the superposition into a thin band.

2.5 Why Overlap Changes Gravity

Ordinary gravity already responds to mass — more mass means stronger gravitational pull. But it does so in a way that always produces the same spatial pattern: in three-dimensional space, gravitational force falls off as the inverse square of distance. Double the distance, quarter the pull. This is true regardless of how much mass is present.

Overlap produces a qualitatively different effect. Because the superimposed bit projections are concentrated into a thin layer — essentially a two-dimensional structure — the additional conservative acceleration field that emerges from their collective structure follows two-dimensional rather than three-dimensional rules. In two dimensions, force falls off as the inverse of distance, not the inverse square. Double the distance, halve the pull — a much lesser decline.

This is precisely the pattern seen in galaxy rotation curves: stars at the outer edges of disk galaxies experience a gravitational pull that declines far more gradually than inverse-square gravity predicts. The standard explanation invokes an invisible halo of dark matter to provide the extra pull. The VERSF explanation is that the pull is real but its source is not a substance — it is the geometric consequence of overlapping bit projections in the disk, producing an effectively two-dimensional gravitational structure embedded in three-dimensional space.

2.6 Summary of the Physical Picture

The mechanism has four layers:

1. **Mass generates irreversible commitments** (bits) that advance time and project their influence outward.
2. **Bit projections propagate** through surrounding space, carrying informational structure beyond the matter that produced it.
3. **Quantum foam is the reversible, temporally sterile medium** through which projections travel. It mediates and constrains propagation but does not create or amplify bit activity.
4. **Overlap occurs where projections from different sources superimpose**, increasing effective information density. In a disk galaxy, geometry concentrates this overlap into a

thin band in the midplane — and the two-dimensional character of that band produces a gravitational scaling that matches what we observe.

What dark matter models attribute to an invisible substance, VERSF attributes to the geometry of overlapping information.

A note on energy. The overlap contribution does not create energy; it redistributes existing commitment structure. Section 6.6 provides a rigorous energy accounting showing that tracers move in a conservative potential derived from a variational principle, with screening preventing runaway amplification.

---

3. TPB Overlap and the Synchronisation Order Parameter

For the general reader: Section 2 described how bit projections from many sources overlap in the disk midplane. To do physics with this picture, we need a mathematical language for "how much overlap is happening at each point" and "how aligned is the overlap pattern from place to place." That language comes from condensed matter physics — the same mathematics used to describe superconductors and superfluids, where large-scale quantum ordering produces dramatic macroscopic effects. The key object is a *complex order parameter* Ψ: its size tells us how strong the overlap coherence is, and its phase angle tells us how the pattern is aligned relative to its neighbours.

3.1 The TPB Commitment Scalar

Let $\tau(\mathbf{x})$ denote the TPB commitment scalar: a coarse-grained measure of irreversible commitment density at spacetime point $\mathbf{x}$. In regions of high baryonic density, τ is large; in intergalactic voids, τ approaches its background value.

A clarification on status: in the TPB framework, what we call "proper time" is itself emergent — it is not a fundamental background parameter but arises from the accumulated commitment structure. The scalar τ is therefore an *operational* quantity: a coarse-grained commitment density as registered by subsystems embedded in the local environment. It is not defined against any fundamental temporal backdrop. This operational definition is sufficient for the coarse-grained Landau–Ginzburg treatment that follows, and no reference to a fundamental time coordinate is required. (In subsequent sections, we write $\bar{\tau}$ for τ coarse-grained on the Landau–Ginzburg cell scale; the distinction is notational, not physical.)

3.2 Complex Order Parameter for Overlap Coherence

At coarse-grained scales, TPB overlap synchronisation is captured by a complex order parameter:

$$\Psi(\mathbf{x}) = f(\mathbf{x})\, e^{i\theta(x)} \quad (6)$$

where $f \geq 0$ is the coherence amplitude and θ is the overlap phase. The amplitude measures the *degree* of coherent overlap — the formal counterpart of the constructive superposition of bit projections described in Section 2; the phase encodes the *relative alignment* of the coherent overlap pattern across space.

This representation carries a U(1) symmetry: the physics is invariant under a global shift $\theta \to \theta +$ const, reflecting the fact that the absolute alignment of the coherent overlap pattern is not physically meaningful — only gradients in the phase (differences in alignment between locations) carry physical content.

The physical identification of this U(1) symmetry is as follows. In standard condensed matter systems, U(1) symmetry is associated with a conserved charge (particle number in superfluids, Cooper pair number in superconductors). In the TPB framework, the analogous quantity is the *overlap winding number*: the net phase accumulated around a closed loop in the coherent region. In the source-free sector, the phase supports topological winding, and single-valuedness of the physical state constrains the winding number to integer values. In the presence of sources (Section 5), the U(1) is explicitly broken: sources select a preferred phase configuration and can permit defect nucleation and annihilation at the boundaries of the coherence band. The winding number is therefore a good quantum number only in the approximate symmetry regime, far from sources and boundaries.

---

4. Deriving Coherence Confinement from TPB Physics

For the general reader: This is the central new result of the paper. We show that TPB overlap coherence doesn't fill all of three-dimensional space — it *automatically confines itself* to a thin layer coinciding with the galactic disk, because the raw material for coherence (dense bit-commitment activity from baryonic matter) only exists there. This is like how a layer of ice forms on the surface of a lake: the ordering (crystallisation) only occurs where conditions (temperature) cross a threshold, producing a thin ordered sheet embedded in a disordered bulk. The rest of the paper's results flow from this confinement.

The geometric superposition of bit projections described in Section 2 is now formalised through a Landau–Ginzburg ordering framework. In this mathematical language, "synchronisation" refers to the establishment of a coherent overlap pattern with well-defined phase — the formal counterpart of the constructive superposition of bit projections in the physical picture.

4.1 Three-Dimensional Landau–Ginzburg Functional

We begin in full three-dimensional space — crucially, we do *not* assume confinement to any surface. The static energy functional for the overlap field is:

$$E\_LG^{(3)} = \int d^3x \, [\, \kappa \, |\nabla \Psi|^2 + a(\mathbf{x})|\Psi|^2 + (b/2)|\Psi|^4 \,] \quad (7)$$

with $b > 0$ for stability and $\kappa > 0$ as the stiffness (rigidity) of the overlap field. The parameter $a(\mathbf{x})$ is the effective mass-squared controlling the local ordering tendency.

The structure of this functional is dictated by symmetry. It is the most general U(1)-invariant energy functional containing terms up to quartic order in Ψ and up to two derivatives — the standard Landau–Ginzburg construction. The TPB-specific content enters through the spatial dependence of the coefficient $a(\mathbf{x})$.

(Note: we use E for this static energy functional to distinguish it from the Lorentzian action S used in later sections when dynamical terms are included.)

4.2 Spatially Varying Synchronisation Drive

In the TPB framework, coherence requires sufficient projected commitment density. The effective control parameter $a(\mathbf{x})$ therefore depends on the local commitment density $\bar{\tau}(\mathbf{x})$. Near the ordering threshold, we expand to leading order:

$$a(\mathbf{x}) = a_0 - \eta\, \bar{\tau}(\mathbf{x}) \quad (8)$$

where $a_0 > 0$ is the bare (incoherent) value and $\eta > 0$ is the coupling strength between commitment density and coherence drive. The linearity in $\bar{\tau}$ is the leading-order term in a Taylor expansion about the critical point, following standard Landau theory practice; higher-order corrections are suppressed near threshold.

The physics is immediate:

- Where $\bar{\tau}(\mathbf{x})$ is small (low commitment density): $a(\mathbf{x}) > 0$, the minimum is at $\Psi = 0$ (no coherence).
- Where $\bar{\tau}(\mathbf{x})$ is large (high commitment density): $a(\mathbf{x}) < 0$, the minimum is at $|\Psi|^2 = |a|/b$ (coherent phase with well-defined θ).

The phase field θ is not a physical degree of freedom where $\Psi = 0$. There is no broken-symmetry manifold to support it. Phase transport is therefore automatically confined to the region where the TPB synchronisation drive pushes $a(\mathbf{x})$ below zero.

4.3 Disk Geometry Produces a Thin Coherence Band

In a disk galaxy, the baryonic (and hence TPB commitment) density is strongly concentrated near the midplane $z = 0$ and falls off steeply in the vertical direction. The control parameter therefore takes the form:

$$a(R, z) \approx a_{\text{bulk}} + \Delta a(R)\, g(z/h) \quad (9)$$

where $a_{\text{bulk}} > 0$ is the incoherent bulk value, $\Delta a(R) < 0$ near the disk drives ordering, g is a profile function peaked at $z = 0$ with characteristic width h (the disk scale height), and R is the cylindrical radial coordinate.

There exists a band $|z| < z^*(R)$ around the midplane where $a(R,z) < 0$. Outside this band, $a > 0$ and the vacuum state is $\Psi = 0$. This band is the coherence manifold Σ — not an assumption, but the *support of the ordered phase*, determined by the baryonic distribution through TPB commitment density.

4.4 Amplitude Profile and Phase Localisation

To demonstrate mathematically that the phase mode is confined to Σ, we solve for the equilibrium amplitude profile. Writing $\Psi = f(z)e^{i\theta}$ where $f(z) \geq 0$, and varying the energy functional (7) with respect to f at fixed θ, the full equation includes in-plane Laplacian terms $\nabla_{\parallel}^2 f$. We treat f as depending only on z — justified when the in-plane scale over which f varies (set by the radial gradient of Σ_b, typically ~ R_d ~ kpc) is much larger than the vertical scale (set by h ~ 100 pc), so that $\nabla_{\parallel}^2 f \ll \partial_z^2 f$. In this approximation the amplitude equation reduces to:

$$-\kappa\, \partial z^2\, f + a(z)\, f + b\, f^3 = 0 \quad (10)$$

For a step-like a(z) profile (negative for $|z| < h$, positive for $|z| > h$), this equation has a well-known domain-wall–type solution:

- **Inside the band** ($|z| \lesssim h$): $f(z) \approx f_0 = \sqrt{(|a|/b)}$, the equilibrium coherence amplitude.
- **Outside the band** ($|z| \gg h$): $f(z) \to 0$ exponentially, with decay governed by the bulk healing length $\xi_{bulk} = \sqrt{(\kappa/a_{bulk})}$.

The effective band thickness is $h_{eff} \approx h + \xi_{bulk}$, combining the geometric disk thickness h with the exterior healing tail. For typical galactic parameters where the bulk is strongly disordered (a_{bulk} large), $\xi_{bulk} \ll h$, and the band closely tracks the baryonic disk.

(Note: a distinct interior healing length $\xi_{in} = \sqrt{(\kappa/2|a|)}$ governs the scale of amplitude disturbances *within* the ordered band; it appears in the screening analysis of Section 7. The two lengths are in general different: ξ_{bulk} controls exterior decay, ξ_{in} controls interior coherence.)

4.5 Dimensional Reduction: From 3D to 2D Phase Theory

The phase kinetic term in the 3D energy functional is:

$$\kappa|\nabla\Psi|^2 = \kappa\, f^2(z)\, |\nabla\theta|^2 + \kappa\, |\partial_z f|^2 + 2\kappa\, f(\partial_z f)(\partial_z \theta) + \ldots \quad (11)$$

The coefficient of the phase gradient term, $\kappa f^2(z)$, is the *phase stiffness*. The cross-term $2\kappa f(\partial_z f)(\partial_z \theta)$ vanishes because θ is taken to be the lowest z-mode in the confined band — approximately z-independent across the thin coherence region (justified below, where higher z-dependent phase modes are gapped by the confinement potential and do not contribute at long wavelengths). The pure amplitude gradient term $\kappa|\partial_z f|^2$ contributes to the amplitude sector and does not affect the phase dynamics. Outside the coherence band, $f \to 0$ and the stiffness vanishes: phase gradients cost no energy because the phase is undefined. There is no propagating θ degree of freedom in the bulk.

For the lowest-energy phase mode, θ is approximately uniform across the thin band (justified when h_eff ≪ L_∥, the in-plane wavelength of interest — easily satisfied for galactic-scale dynamics where L_∥ ~ kpc and h_eff ~ 100 pc). Higher z-dependent modes are gapped by the confinement potential and do not contribute at long wavelengths. We therefore write $\theta \approx \theta(R, \varphi)$ and integrate over z:

$$S_\theta^{(3)} \approx \int d^2x_\parallel \int dz\, [K(z)/2]\, |\nabla_\parallel \theta|^2 \quad (12)$$

where $K(z) = 2\kappa f^2(z)$. Performing the z-integration yields the effective 2D phase action:

$$\mathbf{S_\theta^{(2)} = \int d^2x_\parallel\, [K_\Sigma/2]\, |\nabla_\parallel \theta|^2} \quad (13)$$

$$K_\Sigma := \int dz\, K(z) = 2\kappa \int dz\, f^2(z) \quad (14)$$

This is the central result of the derivation: **the 2D phase theory on Σ is not assumed but obtained by integrating out the localised amplitude profile.** In condensed matter language, it is a phase mode (Goldstone in the source-free sector; pseudo-Goldstone once sourced, as discussed in Section 5.1) living on an ordered film embedded in a disordered bulk.

4.6 What Prevents Three-Dimensional Propagation?

The answer, derived above, is physical and sharp:

1. In the 3D bulk where $a > 0$, the vacuum state is $\Psi = 0$.
2. Where $\Psi = 0$, there is no broken U(1) symmetry, no phase manifold S^1, and θ is not a physical field.
3. The only excitations in the bulk are massive amplitude modes with correlation length $\xi_{bulk} = \sqrt{(\kappa/a_{bulk})}$, which decay exponentially and cannot mediate long-range forces.
4. Phase transport — and hence the overlap-induced gravitational effect — is confined to the region where TPB commitment density exceeds the ordering threshold.

This confinement is a consequence of TPB physics (the synchronisation threshold), not of geometry.

Stability. The coherence band is a local minimum of the Landau–Ginzburg energy functional (7): amplitude perturbations about f_0 are gapped (with mass ~ $1/\xi_{in}$), and the band boundaries are stabilised by the smooth transition of a(z) through zero. Small perturbations to the disk structure (e.g., vertical oscillations, spiral density waves) modulate the location of the $a = 0$ surface but do not destabilise the band — they shift Σ adiabatically. Large perturbations (e.g., mergers destroying disk geometry) can of course disrupt the ordered phase entirely, consistent with the framework's prediction that the mechanism operates only in disk-like geometries.

---

5. Phase Dynamics on the Coherence Manifold

For the general reader: Now that we've shown the overlap pattern confines itself to a thin disk, we need to understand what drives it. The answer is the baryonic matter itself: stars and gas in the disk act as "sources" for the overlap phase, much like electric charges act as sources for the electric field. The bit projections from each source (Section 2) collectively shape the phase pattern. The equation governing this pattern turns out to be the same equation that governs electric fields in two-dimensional systems — and two-dimensional electric fields have a very different character from three-dimensional ones.

5.1 Source Coupling from TPB Commitment

The baryonic matter in the disk drives the overlap phase through TPB commitment density. We introduce a source coupling between the projected TPB commitment density $\mathcal{J}$ on Σ and the phase field:

$$S_{src} = \int_\Sigma d^2x \, \sqrt{\gamma}\, \alpha\, \mathcal{J}\, \theta \quad (15)$$

where α is the coupling constant and γ is the determinant of the induced 2D metric on Σ.

Physical motivation for the linear coupling. In standard condensed matter, Goldstone modes typically couple to matter through derivatives ($\partial_a \theta$), not through θ directly. The linear coupling $\alpha\mathcal{J}\theta$ requires specific justification. In the TPB framework, the physical mechanism is analogous to a *chemical potential* coupling: baryonic commitment density acts as an external field that biases the preferred phase value at each location, much as a chemical potential couples linearly to the phase in superfluid hydrodynamics (where the superfluid velocity is $v_s = \nabla\theta$, but the free energy includes a $\mu N \sim \mu\dot{\theta}$ term that is linear in the time-derivative of the phase). Here the role of the chemical potential is played by the static commitment density $\mathcal{J}$, which sets a preferred phase configuration through the energetics of TPB overlap alignment. The coupling is linear in θ because $\mathcal{J}$ acts as an external source that tilts the free-energy landscape, selecting one phase value over others — not because baryons couple to the Goldstone gradient.

A note on symmetry: This linear coupling explicitly breaks the U(1) symmetry $\theta \to \theta + \text{const}$. This is physically appropriate: in the presence of sources, the phase acquires a preferred configuration (the sourced solution), just as an external magnetic field breaks the rotational symmetry of a ferromagnet. The U(1) is a symmetry of the free overlap field; sources select a phase profile. The consequence is that θ is not a true massless Goldstone mode even before the screening term of Section 7 is introduced — the source coupling itself generates a preferred vacuum. We account for this explicitly in the screened phase equation below.

Remark on chemical-potential analogy. In relativistic superfluid hydrodynamics, the chemical potential couples through a derivative term $\mu\, \partial_t \theta$, reflecting canonical conjugacy between number density and phase. In a strictly static equilibrium sector, such a term contributes only through time-boundary structure (or through time-variation of μ). The present paper does not claim literal equivalence to the superfluid coupling; rather, it adopts $\alpha\mathcal{J}\theta$ as the minimal static bias term: $\mathcal{J}$ acts as an external field that tilts the free-energy landscape and selects a preferred phase configuration. The derivative-vs-static distinction becomes essential in a dynamical treatment, which we defer.

5.2 Effective Phase Action and Equation of Motion

Combining the kinetic term (13) with the source term (15), the total effective phase action is:

$$S_\theta = \int_\Sigma d^2x \, \sqrt{\gamma} \, [-(K_\Sigma/2) \, \gamma^{ab} (\partial_a \theta)(\partial_b \theta) + \alpha \, \mathcal{J} \, \theta] \quad (16)$$

where K_Σ is the integrated phase stiffness from Eq. (14).

Note that $\mathcal{J}$ is itself concentrated in the disk, so the z-integration of the source term localises naturally: $\mathcal{J}$ on Σ is the surface-integrated TPB commitment density, which in the static limit is proportional to the baryonic surface density $\Sigma_b(R)$.

Varying with respect to θ yields the Euler–Lagrange equation. For dynamics, the coherence manifold is extended to $\Sigma \times \mathbb{R}$ (spatial disk × emergent time, with the emergent time parameter defined operationally as in §2.1 and §3.1), carrying a (2+1)-dimensional Lorentzian induced metric γ_{ab}. The kinetic term for the phase is taken to be second-order (Klein–Gordon type, giving $\Box_\Sigma \theta$), corresponding to a relativistic dispersion relation $\omega^2 = k^2 + \mu^2$ for phase excitations. A first-order (Schrödinger-type) kinetic term would yield diffusive rather than propagating dynamics; we adopt the second-order form as appropriate for a Lorentz-covariant effective theory.

The choice of Klein–Gordon structure implies propagating phase disturbances on Σ with a characteristic signal velocity set by the effective metric γ_{ab}. In the present static analysis this does not enter; however, in a full dynamical treatment the phase propagation velocity need not coincide with the ambient spacetime light velocity c. If subluminal, the coherence manifold would carry its own causal structure embedded within the larger spacetime. Exploring this causal sector — including potential observational signatures in time-dependent phenomena such as galaxy interactions or bar instabilities — is deferred to future work.

In the covariant form:

$$\Box_\Sigma \theta = (\alpha/K_\Sigma) \, \mathcal{J} \quad (17)$$

where $\Box_\Sigma$ is the d'Alembertian on $\Sigma \times \mathbb{R}$. Throughout this paper we work in the static sector, dropping the ∂_t^2 term. The static equation reduces to the 2D spatial Poisson equation:

$$\mathbf{\nabla^2_{(2)} \, \theta(R) = (\alpha/K_\Sigma) \, \Sigma_b(R)} \quad (18)$$

where $\nabla^2_{(2)}$ is the 2D spatial Laplacian in the disk plane and $\Sigma_b(R)$ is the baryonic surface density.

---

6. Logarithmic Green's Function and Flat Rotation Curves

For the general reader: Here is where the key scaling change appears. In three dimensions, the gravitational potential of a point mass goes as 1/r (giving $1/r^2$ gravity). But in *two* dimensions, the potential of a point source is ln R (a logarithm). The gradient of ln R is 1/R — and a 1/R gravitational force is *exactly* what produces flat rotation curves. By confining the overlap phase to two dimensions, the TPB framework naturally produces the right kind of force law without any fine-tuning and without introducing invisible matter.

6.1 The 2D Green's Function

The Green's function G for the 2D Laplacian satisfies:

$$\nabla^2_{(2)}\, G(\mathbf{R}) = \delta^{(2)}(\mathbf{R}) \quad (19)$$

The standard result, following from the identity:

$$\nabla^2_{(2)} \ln R = 2\pi\, \delta^{(2)}(\mathbf{R}) \quad (20)$$

is:

$$G(\mathbf{R}) = (1/2\pi) \ln R \quad (21)$$

6.2 Phase Solution for Localised Sources

For a source distribution that is localised or that can be treated as approximately point-like at large R, the phase solution is:

$$\theta(R) = (\alpha / 2\pi K\_\Sigma)\, M\_b \ln R + (\text{terms regular at large } R) \quad (22)$$

where $M\_b = \int d^2x\_\| \, \Sigma\_b$ is the total baryonic mass (surface-integrated). At radii much larger than the source extent but within the coherence band, the logarithmic term dominates.

For a more realistic extended source profile $\Sigma\_b(R)$, the full solution is obtained by convolution with the Green's function. The key property is that for *any* localised source, the large-R behaviour is dominated by the logarithmic monopole term, with corrections from the source's multipole structure that fall off with increasing R.

6.3 Gravitational Coupling: From Phase to Effective Potential

Interpretation (effective potential). In this paper, θ is introduced as the long-wavelength phase mode of the TPB overlap order parameter, and Eq. (18) shows that in the disk plane it satisfies a Poisson-type equation sourced by baryonic surface density. We therefore define an overlap-induced contribution to the weak-field gravitational potential by:

$\Phi_{ov} := \lambda\,\theta$ (23)

Minimal tracer coupling and equation of motion. In the weak-field static sector, the observable content of the overlap mechanism is the additional conservative acceleration experienced by baryonic tracers in the disk plane. The most general way to encode such a conservative influence is through an effective potential term in the tracer action:

$$S_{tr} = \int dt \left[\tfrac{1}{2} m v^2 - m \Phi_N(\mathbf{x}) - m \Phi_{ov}(\mathbf{x}) \right] \quad (24)$$

We define the overlap-induced potential as $\Phi_{ov} := \lambda\theta$, where θ is the unique long-wavelength overlap phase mode satisfying the sourced 2D Poisson equation on Σ (Eq. 18). Varying S_{tr} yields the equation of motion:

$$\mathbf{a} = -\nabla\Phi_N - \nabla\Phi_{ov} = -\nabla\Phi_N - \lambda\,\nabla\theta \quad (25)$$

Thus, once θ is determined by baryonic surface density via Eq. (18), the overlap-induced acceleration follows immediately. The coefficient λ is an effective coupling converting overlap-phase units to conventional potential units; deriving λ from the microscopic VERSF gravitational sector is deferred to future work. Here λ is treated as a phenomenological calibration parameter constrained by rotation curve data and by the requirement that deviations from standard gravity at Solar System scales are negligible.

Crucially, θ is not assumed to source the Einstein equations directly. The effective potential Φ_{ov} is defined operationally via the acceleration it induces on baryonic tracers in the disk plane, independent of any specific metric interpretation. It is an emergent auxiliary field whose geometric scaling (how it depends on R) is a consequence of 2D Poisson structure alone, while the normalisation (how large the effect is) is set by λ. This separation of shape from normalisation is standard practice in effective field theory treatments of modified gravity.

Remark (covariant completion). A full covariant completion would promote Ψ (or θ in the phase-only regime) to a dynamical field with stress-energy:

$$T_{ab}^{(ov)} = K_\Sigma \left[(\partial_a \theta)(\partial_b \theta) - \tfrac{1}{2} \gamma_{ab} (\partial_c \theta)(\partial^c \theta) \right] \quad (26)$$

and compute its backreaction on the metric through the Einstein equations. That calculation is not required to establish the existence and geometric scaling of the 1/R regime, which follows from the confined phase Poisson equation alone. The covariant route would in principle determine λ from first principles; we defer this to future work within the broader VERSF gravitational sector.

6.4 Flat Rotation Curves

With $\Phi_{ov} \propto \ln R$, the overlap-induced acceleration is:

$$a_{ov}(R) = |\partial_R \Phi_{ov}| = (\lambda\alpha\, M_b) / (2\pi K_\Sigma) \cdot (1/R) \quad (27)$$

The circular orbital velocity satisfies $v^2(R) = R \cdot a(R)$. In the regime where the overlap contribution dominates over the Newtonian $1/R^2$ term:

$v^2(R) \approx v_\infty^2 = (\lambda\alpha\, M_b) / (2\pi K_\Sigma) = \text{constant}$ (28)

This is the flat rotation curve, obtained without dark matter. The asymptotic velocity depends on the total baryonic mass M_b and the ratio of coupling constants $\lambda\alpha/K_\Sigma$.

6.5 The Baryonic Tully–Fisher Relation as a Stiffness Scaling Constraint

The baryonic Tully–Fisher relation (BTFR) is the empirical observation that $M_b \propto v_\infty^4$ for disk galaxies (McGaugh, Lelli & Schombert 2016), with a universal proportionality constant involving a single acceleration scale $a_0 \approx 1.2 \times 10^{-10}$ m/s². Any framework claiming to address rotation curves must confront it.

Proposition (BTFR Consistency Condition). From Eq. (28), $v_\infty^2 \propto M_b/K_\Sigma$. Therefore BTFR ($M_b \propto v_\infty^4$) holds if and only if:

$K_\Sigma \propto \sqrt{M_b}$ (equivalently, $\lambda\alpha/K_\Sigma \propto M_b^{-1/2}$) (29)

This makes BTFR a constraint on how coherence stiffness scales with baryonic mass and disk structure — not an automatic consequence of 2D logarithmic propagation, and not an afterthought.

Emergent acceleration scale. In the BTFR-consistent regime, write $K_\Sigma = k_* \sqrt{M_b}$ where k_* is the proportionality constant. Substituting into Eq. (28):

$$v_\infty^4 = (\lambda\alpha / 2\pi k_*)^2 M_b$$

Define an effective acceleration scale:

$$G\, a_{TPB} := (\lambda\alpha / 2\pi k_*)^2 \quad (30)$$

so that:

$$v_\infty^4 = G\, a_{TPB}\, M_b \quad (31)$$

This has the same algebraic form as the MOND relation $v_\infty^4 = G\, a_0\, M_b$ (Milgrom 1983). The acceleration scale a_{TPB} is not inserted by hand but encodes the stiffness normalisation k_* and the coupling product $\lambda\alpha$. Whether a_{TPB} matches the observed value $a_0 \approx 1.2 \times 10^{-10}$ m/s² is a quantitative constraint on these parameters — a target for future TPB microphysical modelling, not a free tuning.

TPB-native route to the scaling. The stiffness is $K_\Sigma = 2\kappa \int dz\, f^2(z) \sim f_0^2\, h_{eff}$, with $f_0^2 = |a|/b$ and $a = a_0 - \eta\bar{\tau}$. In disk galaxies, $\bar{\tau}$ (hence a) is controlled by baryonic surface density and crosses the ordering threshold $a = 0$ at a radius R_* defined by:

$\Sigma(R_*) = \Sigma_{crit}$ (32)

where $\Sigma_{crit} := a_0/\eta$ is a universal coherence threshold surface density (analogous to the Toomre threshold in disk stability; Toomre 1964). For an exponential disk $\Sigma(R) = \Sigma_0 \exp(-R/R_d)$, this gives:

$R_* = R_d \ln(\Sigma_0/\Sigma_{crit})$ (33)

This threshold geometry ties K_Σ to disk scale length and thickness rather than to baryonic mass alone. If disks self-regulate to hover near a universal coherence threshold (so that $|a|$ is approximately constant across galaxies and the scaling comes primarily from h_{eff} and the radial extent of the coherent band), then under observed disk size–mass scalings (Shen et al. 2003; van der Wel et al. 2014) and weakly varying scale height, $K_\Sigma \propto \sqrt{M_b}$ is plausible.

The physical picture is that K_Σ is not a free parameter but is set by *threshold geometry*: ordering occurs only where $\bar{\tau}$ exceeds a critical value, so the coherent region's size and stiffness are determined by where and how deeply the disk crosses threshold. This makes the BTFR a statement about disk structure, not a coincidence.

Falsifiable predictions from stiffness scaling. The BTFR slope is a direct empirical diagnostic of how K_Σ scales with M_b:

- If $K_\Sigma \propto \sqrt{M_b}$, then BTFR holds with slope 4 (the observed value).
- If K_Σ scales closer to M_b, slope drifts toward 2.
- If K_Σ is nearly constant across galaxies, slope drifts toward 1.

The framework further predicts that BTFR scatter should correlate with disk thickness h, central surface density Σ_0, and gas fraction — through their influence on K_Σ and R_*. This provides concrete observational targets: galaxies with anomalously thick disks or low surface density should show systematic deviations from the mean BTFR, in a direction and magnitude predictable from the threshold geometry.

The threshold surface density as an observable. The parameter $\Sigma_{crit} = a_0/\eta$ packages two microscopic parameters into a single phenomenological scale. In principle it is directly observable: it corresponds to the baryonic surface density at which rotation curves begin to deviate systematically from Keplerian behaviour — i.e., the surface density at which TPB coherence "turns on." Empirically, disk galaxies exhibit a characteristic central surface brightness (Freeman 1970; $\Sigma_0 \approx 140\ M_\odot\ pc^{-2}$), suggesting a natural comparison scale. Determining whether Σ_{crit} clusters around the Freeman value, or varies systematically with morphology and gas fraction, provides a direct observational test of the TPB coherence threshold and constrains the microscopic coupling η.

6.6 Energy Accounting and Conservation

Energy is not created; it is redistributed. The overlap mechanism introduces an additional conservative acceleration field in the disk plane. Any conservative force admits a potential

representation and therefore a conserved mechanical energy for tracers. In the present framework, the total effective potential is:

$\Phi_{tot}(\mathbf{x}) = \Phi_N(\mathbf{x}) + \Phi_{ov}(\mathbf{x})$, $\Phi_{ov} := \lambda\theta$

A baryonic tracer of mass m moving in the static potential Φ_{tot} has conserved energy:

$E = (1/2)\, m\, v^2 + m\, \Phi_{tot}(\mathbf{x})$

so long as the fields are time-independent (the regime treated in this paper). The overlap contribution does not violate energy conservation at the level of test-particle dynamics: it modifies the potential landscape but does not inject energy into the tracer system.

Where the "energy" lives. The phase field θ arises from an ordered overlap mode and carries an effective stiffness energy on Σ. From the 2D phase action (Eq. 16), one may define the corresponding static free-energy functional (up to a constant):

$F_\theta[\theta] = \int d^2x_{\parallel} \sqrt{\gamma}\, [\, (K_\Sigma/2)\, (\nabla\theta)^2 - \alpha\, \mathcal{J}\, \theta\,]$

The sourced Poisson equation (Eq. 18) is precisely the Euler–Lagrange condition $\delta F_\theta/\delta\theta = 0$. The θ configuration is the equilibrium profile that minimises the overlap free energy given the baryonic source distribution. The overlap contribution is therefore not an extra reservoir of energy; it is the macroscopic manifestation of how existing commitments organise the substrate's distinguishability structure at minimum free energy.

No runaway amplification. The screening term (Section 7) adds a positive contribution $(K_\Sigma \mu^2/2)\theta^2$ to F_θ, making the free energy strictly convex in the infrared and preventing unbounded growth of θ. Beyond the coherence length, further phase deformation is exponentially costly, and the overlap potential decays. This ensures that the overlap field does not lead to runaway long-range amplification.

Covariant accounting (deferred). A fully covariant completion would treat Ψ (or θ) as part of the gravitational sector and specify how its free-energy functional maps into spacetime stress-energy and lensing potentials. That embedding is deferred. However, within the static disk regime studied here, energy conservation is explicit: tracers move in a conservative potential, and the overlap phase profile is determined by a variational principle minimising a well-defined free-energy functional.

---

7. Coherence Length, Screening, and the Outer Cutoff

For the general reader: The flat rotation curve can't extend forever — eventually the overlap coherence must fade. The Landau–Ginzburg framework provides a natural length scale, the "coherence length," beyond which the overlap effect weakens. This gives the model a built-in outer edge without needing to be added by hand.

7.1 Coherence (Healing) Length

Linearising the amplitude equation (10) about the equilibrium value f_0 gives the interior healing length:

$$\xi_{in} = \sqrt{(\kappa / 2|a|)} \quad (34)$$

(The factor of 2 arises from the curvature of the Mexican-hat potential at its minimum: $V''(f_0) = 2|a|$.) This sets the scale over which amplitude disturbances heal within the ordered band. Identifying ξ_{in} as the in-plane screening scale ($\mu \approx 1/\xi_{in}$) assumes isotropic stiffness κ — i.e., that the Landau–Ginzburg gradient coefficient is the same in the vertical and in-plane directions. Under this assumption, the same parameter that governs vertical amplitude healing also sets the in-plane scale at which phase correlations begin to weaken. (Recall from Section 4.4 that the distinct bulk healing length $\xi_{bulk} = \sqrt{(\kappa/a_{bulk})}$ governs exterior decay.)

7.2 Screened Phase Equation

At in-plane distances comparable to ξ_{in}, phase correlations decay. An effective description incorporates this through a mass term for the phase:

$$S_\theta \rightarrow S_\theta - \int_\Sigma d^2x_\parallel \sqrt{\gamma}\, (K_\Sigma \mu^2/2)\, \theta^2 \quad (35)$$

The screening mass μ receives contributions from two physically distinct sources:

- **Finite coherence length** (Landau–Ginzburg origin): amplitude fluctuations at the edge of the coherent band generate an effective mass $\mu_{LG} \sim 1/\xi_{in}$ for the phase, scaling as $\sqrt{(|a|/\kappa)}$. This is intrinsic to the ordered phase and is present even without sources.
- **Explicit U(1) breaking** (source origin): the linear coupling $\alpha\mathcal{J}\theta$ (Eq. 15) generates a preferred phase vacuum, producing an effective mass μ_{src} that depends on the source strength and coupling constant.

In the galactic context, the Landau–Ginzburg contribution is expected to dominate. The reason is that μ_{LG} is set by the coherence physics of the ordered band — a bulk property of the phase — while μ_{src} is proportional to $\alpha\mathcal{J}$, which is the small perturbative coupling that sources the phase in the first place. If the sourcing were strong enough for μ_{src} to dominate, the linear-response (Poisson) treatment of the phase equation would break down. Consistency of the perturbative framework therefore requires $\mu_{src} \ll \mu_{LG}$, and we identify $\mu \approx \mu_{LG} \approx 1/\xi_{in}$ as the leading contribution.

The screened phase equation is:

$$\mathbf{(\nabla^2_{(2)} - \mu^2)\, \theta(R) = (\alpha/K_\Sigma)\, \Sigma_b(R)} \quad (36)$$

7.3 Screened Green's Function and Rotation Curve Profile

The Green's function for the screened 2D equation is the modified Bessel function K_0:

$G_\mu(R) = -(1/2\pi)\, K_0(\mu R)$ (37)

The asymptotic behaviour is:

- **$\mu R \ll 1$** (inside the coherence band): $K_0(\mu R) \approx -\ln(\mu R/2) - \gamma_E$, recovering the logarithmic regime and flat rotation curves.
- **$\mu R \gg 1$** (beyond the coherence band): $K_0(\mu R) \approx \sqrt{(\pi/2\mu R)} \cdot \exp(-\mu R)$, giving exponential decay and a return toward Keplerian fall-off.

The transition occurs at $R \sim 1/\mu \approx \xi_{in}$, providing a natural outer boundary for the flat rotation curve regime without fine-tuning.

---

8. Effective Halo Mapping

For the general reader: If a conventional astronomer tried to explain the overlap-induced gravitational effects using only standard physics, they would be forced to invent an invisible halo of matter with a very specific density profile — falling off as $1/R^2$. This is precisely the "isothermal halo" that dark matter models invoke. In other words, what dark matter models describe as a physical substance, VERSF describes as the gravitational shadow of two-dimensional phase coherence.

8.1 Rewriting in Local Poisson Form

If one insists on describing the total gravitational potential through the local 3D Poisson equation, one must define an effective source density:

$\nabla^2 \Phi_{total} = 4\pi G\, (\rho_b + \rho_{eff})$ (38)

The overlap contribution Φ_{ov} is defined on the 2D disk Σ. The actual 3D gravitational potential generated by a surface distribution is obtained by solving the 3D Laplace equation with boundary conditions set by the surface values. The result is smooth off-plane, not distributional: at height z above the disk, the logarithmic in-plane behaviour transitions to 3D (1/r) behaviour over a vertical scale comparable to the in-plane wavelength. Specifically, for a surface potential $\Phi_{ov}^{(2D)}(R) \propto \ln R$ on the disk, the 3D continuation satisfies:

$\Phi_{ov}(R, z) \to \Phi_{ov}^{(2D)}(R)$ as $z \to 0$, $\Phi_{ov}(R, z) \to -GM/\sqrt{(R^2 + z^2)}$ as $|z| \to \infty$ (39)

The logarithmic regime and its associated 1/R acceleration hold strictly in the disk plane; off-plane, the potential smoothly crosses over to standard 3D behaviour. This has direct implications for gravitational lensing predictions (since photon trajectories generally do not remain in the disk plane) and for dynamical tracers with significant vertical excursions. A full treatment of lensing and off-plane dynamics requires solving the 3D boundary-value problem with the surface potential as input, which we defer to future work. For the rotation curve analysis (circular orbits in the midplane), the 2D treatment is exact. (In the strict thin-disk limit one may approximate the

surface source by a δ(z) distribution; however, the physically correct continuation is smooth off-plane as a solution of the 3D boundary-value problem.)

8.2 The Isothermal Profile via Spherically Averaged Mass

The correct route to the effective halo density is not the 3D Laplacian of ln R (which is a distributional object with different structure), but the standard *spherically averaged mass profile* interpretation used in observational astronomy.

In the flat rotation curve regime, $a(R) = v_\infty^2/R$. By the Gauss-law / enclosed-mass argument:

$$M_{eff}(R) = (v_\infty^2/G)\, R \quad (40)$$

The effective mass enclosed within radius R grows linearly. The spherically averaged density profile that produces this enclosed mass is:

$$\rho_{eff}(R) = [1/(4\pi R^2)]\, dM_{eff}/dR = v_\infty^2 / (4\pi G R^2) \quad (41)$$

This is the *isothermal halo* profile — the standard dark matter density profile used to fit flat rotation curves. It is the spherically averaged effective density that a conventional Newtonian analysis would attribute to an unseen mass component producing the observed 1/R acceleration.

The isothermal profile has a well-known pathology: the total enclosed mass $M_{eff}(R) \propto R$ diverges linearly, so the integrated mass is infinite. In standard CDM, this is resolved by the NFW profile's outer fall-off (Navarro, Frenk & White 1997). In the present framework, the divergence is resolved by the screening mechanism of Section 7: the screened Green's function (Eq. 37) transitions from logarithmic to exponentially decaying at $R \sim 1/\mu$, so the effective $1/R^2$ density profile is truncated at the coherence radius, yielding a finite total effective mass. The screening thus provides the physical regularisation that the isothermal profile alone lacks.

The VERSF overlap mechanism reproduces the empirical dark matter halo profile as an effective description within the coherence band, with a built-in outer truncation: what conventional gravity interprets as a $1/R^2$ density distribution of physical particles, the TPB framework identifies as the gravitational signature of two-dimensional phase coherence on the disk.

---

9. Regime of Validity and Limitations

For the general reader: Every good theory should be honest about where it works and where it doesn't. This mechanism relies on having a thin, ordered layer — which disk galaxies naturally provide. But elliptical galaxies and galaxy clusters don't have this structure, so the mechanism won't straightforwardly explain their dark matter phenomenology. That's not a fatal flaw — it defines the regime where this particular VERSF effect operates, and other mechanisms may be relevant elsewhere.

9.1 Geometry Dependence

The derivation in Section 4 relies on two features of disk galaxies:

1. **High midplane commitment density** producing $a(z) < 0$ in a thin band.
2. **Thin-band geometry** ($h_{eff} \ll R$) enabling the dimensional reduction to 2D.

Elliptical galaxies and galaxy clusters do not generically satisfy these conditions. In a roughly spherical matter distribution, $a(\mathbf{x})$ may be driven negative throughout a 3D volume, yielding a 3D coherent phase with a 3D Green's function ($1/r$) rather than the 2D logarithmic one. In this case, the overlap contribution to the potential would not produce flat rotation curves.

This is a *feature*, not a bug: disk galaxies and ellipticals show different dark matter phenomenology observationally, and a framework that treats them differently is potentially more discriminating than one that invokes a universal dark halo.

9.2 Additional Observational Constraints

A complete replacement for dark matter must also address:

- **Galaxy cluster dynamics:** Virial masses, X-ray gas profiles, and the Bullet Cluster morphology.
- **Gravitational lensing:** Strong and weak lensing profiles around galaxies and clusters. Because the overlap-induced potential is confined to a thin coherence band, the effective gravitational field is anisotropic — concentrated in the disk plane rather than distributed in a quasi-spherical halo as in CDM. The framework therefore predicts orientation-dependent lensing signatures: disk galaxies viewed edge-on should exhibit stronger projected lensing asymmetry aligned with the disk plane than face-on systems. A full covariant lensing calculation requires solving the Einstein equations with the overlap stress-energy included (or, equivalently, the 3D boundary-value problem of §8.1) and lies beyond the present scope. However, the geometric anisotropy is a clear qualitative discriminator between this mechanism and spherical dark matter halos.
- **Cosmic Microwave Background:** The acoustic peak structure, which in ΛCDM is sensitive to the dark matter density.
- **Structure formation:** The growth of large-scale structure from primordial perturbations.

The present paper does not address these; its scope is limited to providing an internally consistent structural mechanism for flat rotation curves in disk galaxies within the VERSF–TPB framework. Extension to the above domains is a programme for future work.

9.3 Falsifiability

The framework makes several concrete, testable predictions that distinguish it from standard cold dark matter (CDM) models:

1. **Geometry dependence:** The mechanism predicts qualitatively different dark matter phenomenology for disk vs. non-disk galaxies, tied to the existence (or absence) of a thin coherence band.
2. **Correlation with disk structure:** The onset and extent of the flat rotation curve regime should correlate with disk scale height h and surface density (through the coherence threshold a = 0).
3. **Transition profile:** The screened Green's function (Section 7.3) predicts a specific functional form for the transition from flat to Keplerian at large R, governed by a single parameter μ, which differs from the NFW (Navarro, Frenk & White 1997) or Burkert (1995) profiles used in CDM.
4. **Scaling relations:** The prediction $v_\infty^2 \propto M_b$ (before possible mass-dependent corrections to K_Σ) differs from the MOND prediction of $v_\infty^4 \propto M_b$ and from CDM predictions that depend on halo concentration.

Of these, the cleanest near-term discriminator is prediction (3): the transition profile governed by the single parameter μ yields a specific functional form (modified Bessel K_0) that differs from the NFW (Navarro, Frenk & White 1997), Burkert (1995), and isothermal profiles used in standard dark matter fits, and can be tested against high-quality extended rotation curve data.

9.4 Pre-emptive Clarifications and Scope Boundaries

This subsection addresses predictable objections and delineates precisely what is and is not claimed.

9.4.1 Scope and status of the mechanism. The present mechanism does not modify Newton's law or General Relativity universally. The 1/R regime arises only in geometries that support a thin coherence band — specifically, disk galaxies in which $a(\mathbf{x}) < 0$ in a narrow midplane region. In approximately spherical systems (e.g., the Solar System), coherence would extend in three dimensions, the Green's function reverts to the standard 3D 1/r form, and no deviation from tested dynamics is predicted. The mechanism is regime-specific, not universal. No new particle species are introduced; the overlap field Ψ is a coarse-grained order parameter, and the phase mode θ arises only where the ordering threshold is crossed. The identification $\Phi_{ov} := \lambda\theta$ (Section 6.3) is an effective description in the static weak-field disk sector: the shape of the effect (logarithmic potential, 1/R acceleration) is derived from 2D Poisson structure; the normalisation λ is phenomenological. A full covariant derivation promoting Ψ to a dynamical field and solving Einstein's equations for backreaction is beyond the present scope.

9.4.2 Lensing implications. Because the overlap-induced potential is confined to a thin disk-aligned band, the framework predicts anisotropic gravitational effects contrasting with quasi-spherical CDM halos. Qualitatively: disk galaxies viewed edge-on should exhibit stronger projected deflection aligned with the disk plane; face-on systems should show reduced projected asymmetry. A full lensing calculation requires solving the Einstein equations with the overlap stress-energy included (cf. the 3D boundary-value problem of §8.1) and lies beyond the present scope. However, geometric anisotropy is a robust qualitative discriminator between the TPB overlap mechanism and spherical halo models.

9.4.3 The role of the coherence threshold Σ_crit. The threshold surface density Σ_crit = a_0/η is a phenomenological parameter packaging microscopic constants of the TPB ordering mechanism. In principle, Σ_crit is directly measurable: it corresponds to the baryonic surface density at which rotation curves begin to deviate from Keplerian behaviour. Its relationship to empirical disk surface density scales (e.g., Freeman 1970) provides a direct observational test of the framework (see §6.5).

9.4.4 On the baryonic Tully–Fisher relation. The recovery of the BTFR requires a specific scaling of the integrated stiffness K_Σ with baryonic mass. This is not assumed but identified as a constraint on the TPB microphysics (§6.5). If disk size–mass and scale-height relations satisfy the conditions outlined there, BTFR follows with slope 4. If not, the mechanism predicts deviations from slope 4. The BTFR therefore functions as a quantitative diagnostic of how coherence stiffness scales with galactic structure.

9.4.5 Scope of the present work. This paper provides a structural mechanism for flat rotation curves in thin disk galaxies within the VERSF–TPB framework. It does not claim: (a) a universal replacement for dark matter in all astrophysical contexts, (b) a completed covariant lensing solution, or (c) a full cosmological structure-formation model. Those extensions require further development of the VERSF gravitational sector.

Closing remark. The central claim is narrow and testable: in geometries that support a thin TPB coherence band, the confined phase mode produces a logarithmic Green's function whose 1/R acceleration profile matches flat rotation curves. When interpreted through standard 3D gravity, this appears as an isothermal halo.

---

10. Summary and Conclusions

We have presented a structural mechanism within the VERSF–TPB framework by which flat galactic rotation curves arise from phase-coherent overlap dynamics rather than dark matter particles. The argument proceeds through five steps:

Step 1 (Section 1): Local vacuum geometry in 3D produces $1/r^2$ gravitational acceleration, which is incompatible with flat rotation curves. An additional source or an effective dimensional reduction is required.

Step 2 (Sections 2–3): The physical picture of bit projection and overlap is introduced (Section 2), and TPB overlap synchronisation is formalised through a complex order parameter Ψ with U(1) symmetry (Section 3), whose amplitude measures coherence and whose phase θ is the long-range degree of freedom.

Step 3 (Section 4): Starting from a 3D Landau–Ginzburg energy functional with a spatially varying commitment-driven ordering control parameter $a(\mathbf{x})$, we derive that coherence is confined to a thin band Σ coinciding with the galactic disk. The phase mode is a localised surface excitation — a Goldstone mode of the free overlap field (pseudo-Goldstone under sourcing)

living on an ordered film in a disordered bulk. This gives a 2D effective phase theory without assuming 2D.

Step 4 (Sections 5–6): The sourced 2D phase equation has a logarithmic Green's function, yielding $\Phi_{ov} \propto \ln R$, acceleration $\propto 1/R$, and flat rotation curves $v \approx v_\infty$ = constant.

Step 5 (Section 7): A screening mass from finite coherence length provides a natural outer cutoff, beyond which rotation curves return toward Keplerian fall-off.

The effective density profile that conventional gravity would attribute to this mechanism is $\rho_{eff} \propto 1/R^2$ — the isothermal halo. No new particles are introduced. The mechanism is specific to geometries supporting thin ordered bands, which provides falsifiable predictions distinguishing it from universal dark matter models.

References

- **Burkert, A.** (1995). "The Structure of Dark Matter Halos in Dwarf Galaxies." *Astrophysical Journal Letters*, 447, L25.
- **Clowe, D., Bradač, M., Gonzalez, A. H., Markevitch, M., Randall, S. W., Jones, C. & Zaritsky, D.** (2006). "A Direct Empirical Proof of the Existence of Dark Matter." *Astrophysical Journal Letters*, 648, L109.
- **Freeman, K. C.** (1970). "On the Disks of Spiral and S0 Galaxies." *Astrophysical Journal*, 160, 811.
- **McGaugh, S. S., Lelli, F. & Schombert, J. M.** (2016). "Radial Acceleration Relation in Rotationally Supported Galaxies." *Physical Review Letters*, 117, 201101.
- **Milgrom, M.** (1983). "A Modification of the Newtonian Dynamics as a Possible Alternative to the Hidden Mass Hypothesis." *Astrophysical Journal*, 270, 365–370.
- **Navarro, J. F., Frenk, C. S. & White, S. D. M.** (1997). "A Universal Density Profile from Hierarchical Clustering." *Astrophysical Journal*, 490, 493–508.
- **Shen, S., Mo, H. J., White, S. D. M., Blanton, M. R., Kauffmann, G., Voges, W., Brinkmann, J. & Csabai, I.** (2003). "The Size Distribution of Galaxies in the Sloan Digital Sky Survey." *Monthly Notices of the Royal Astronomical Society*, 343, 978–994.
- **Toomre, A.** (1964). "On the Gravitational Stability of a Disk of Stars." *Astrophysical Journal*, 139, 1217–1238.
- **van der Wel, A., Franx, M., van Dokkum, P. G., Skelton, R. E., Momcheva, I. G., Whitaker, K. E., Brammer, G. B., Bell, E. F., Rix, H.-W., Wuyts, S., et al.** (2014). "3D-HST+CANDELS: The Evolution of the Galaxy Size-Mass Distribution since z = 3." *Astrophysical Journal*, 788, 28.

Appendix A: Notation and Conventions

Symbol	Definition
$G_{\mu\nu}$	Einstein tensor
$T_{\mu\nu}$	Stress-energy tensor
Φ	Newtonian gravitational potential
$\tau(\mathbf{x})$	TPB commitment scalar (coarse-grained commitment density)
$\Psi = f \cdot e^{i\theta}$	Overlap order parameter
f	Coherence amplitude
θ	Overlap phase
Σ	Coherence manifold (support of ordered phase)
γ_{ab}	Induced metric on Σ
κ	Overlap field stiffness
$a(\mathbf{x})$	Commitment-driven ordering control parameter
b	Quartic stabilisation coefficient
K_Σ	Integrated phase stiffness on Σ
α	Phase-source coupling constant
λ	Overlap-gravity coupling constant
μ	Screening mass ($\approx 1/\xi_{in}$)
ξ_{in}	Interior coherence (healing) length
ξ_{bulk}	Bulk (exterior) healing length
$\mathcal{J}$, Σ_b	TPB commitment density, baryonic surface density

Units: Natural units $c = \hbar = 1$ unless stated otherwise. Metric signature $(-,+,+,+)$.

Appendix B: Detailed Derivation of the Amplitude Equation

Starting from the energy functional (7) with $\Psi = f(z)\, e^{i\theta(R,\varphi)}$, and applying the z-only approximation for f justified in §4.4 ($\nabla_\parallel^2 f \ll \partial_z^2 f$), the variation $\delta E/\delta f = 0$ gives:

$$-2\kappa\, \partial z^2\, f + 2a(z)\, f + 2b\, f^3 = 0$$

Dividing by 2:

$$-\kappa\, \partial z^2\, f + a(z)\, f + b\, f^3 = 0 \quad \text{(B1)}$$

For a step-function profile $a(z) = -|a|$ for $|z| < h$ and $a(z) = a_{bulk}$ for $|z| > h$:

Interior ($|z| < h$): Setting $\partial^2_z f \approx 0$ (uniform solution), we get $-|a|f + bf^3 = 0$, yielding $f_0 = \sqrt{(|a|/b)}$.

Exterior ($|z| > h$): Linearising about $f = 0$, the equation becomes $-\kappa\, \partial^2_z f + a_{bulk} f = 0$, with decaying solution $f \propto e^{(-|z|/\xi_{bulk})}$ where $\xi_{bulk} = \sqrt{(\kappa/a_{bulk})}$.

Matching region ($|z| \approx h$): The amplitude interpolates smoothly between f_0 and 0 over a characteristic width $\xi_{in} = \sqrt{(\kappa/2|a|)}$, the interior healing length (the factor of 2 reflects the curvature $V''(f_0) = 2|a|$ of the potential at its minimum, as in Eq. (34)). We use ξ_{in} as an order-of-magnitude width for the interface; precise numerical prefactors depend on the detailed smooth profile of $a(z)$. The full domain-wall–type interpolating solution can be obtained analytically for specific smooth $a(z)$ profiles (e.g., hyperbolic tangent) but the qualitative structure — flat interior, exponential exterior, smooth matching — is universal.

Appendix C: Beyond Disk Rotation Curves — Clusters, Lensing, CMB, and Structure Formation

This appendix clarifies how the disk-coherence mechanism developed in the main text interfaces with the broader empirical roles commonly attributed to dark matter: galaxy cluster dynamics, gravitational lensing, CMB acoustic peaks, and large-scale structure formation. The purpose is not to claim completion of these domains, but to (i) state precisely what the present paper does and does not imply, (ii) identify the minimal extensions required for coverage, and (iii) define falsifiable intermediate targets.

C.1 Scope of the Main Mechanism

The main paper establishes a specific result: in geometries supporting a thin TPB coherence band (disk galaxies), confinement of the overlap phase mode produces a 2D Poisson equation with logarithmic Green's function and thus a $1/R$ acceleration regime, with a screening cutoff at scale $R \sim \mu^{-1}$ (Section 7).

This mechanism is not claimed to be universal. It is activated only when the ordering condition $a(\mathbf{x}) < 0$ occurs in a thin band (Section 4.3). In systems lacking this geometry (e.g., clusters), the overlap phase is not expected to be confined in the same way, and the 2D logarithmic regime should not be assumed.

C.2 Cluster Mass Discrepancy: What Must Be Explained

Galaxy clusters exhibit mass discrepancies inferred from virial equilibrium of member galaxies, X-ray temperature and density profiles of intracluster gas, and strong and weak gravitational lensing including merging systems (e.g., the Bullet Cluster; Clowe et al. 2006).

Any full alternative to particle dark matter must provide a gravitational field sufficient to reproduce cluster lensing convergence maps, reproduce hydrostatic equilibrium profiles, and maintain consistency across dynamical and lensing estimators. The present paper does not provide this.

However, it does provide a framework for how such effects could arise without new particles: through ordered overlap phases supported by the local sign structure of $a(\mathbf{x})$.

C.3 Cluster Regime Hypothesis: 3D Ordering Rather Than Disk Confinement

In clusters, baryons are distributed approximately three-dimensionally (gas dominates the baryonic mass budget). Within TPB, this suggests a different ordering morphology:

- **In disks:** $a(\mathbf{x}) < 0$ in a thin midplane band → 2D confined phase → logarithmic potential → flat rotation curves (this paper).
- **In clusters:** $a(\mathbf{x}) < 0$ may occur in an extended 3D volume (or in multiple filaments/sheets) → 3D coherent phase → 3D Green's function structure. Whether this occurs depends on whether $\bar{\tau}$ sourced by intracluster gas crosses the ordering threshold throughout a volume rather than in a sheet — a question determined by the gas density profile and the microscopic coupling η.

Consequence. If a 3D ordered overlap phase forms, the relevant Green's function is no longer logarithmic but reverts to the standard $1/r$ form. The resulting acceleration follows the usual $1/r^2$ scaling — the overlap contribution does not change the radial profile but adds to the effective gravitational strength, renormalising G_{eff} upward. This is appropriate to the cluster problem, which is fundamentally a *magnitude* discrepancy (not enough gravitational mass to explain observed binding) rather than a *scaling* discrepancy (wrong radial dependence). The cluster regime therefore requires its own analysis: the disk mechanism should not be naively extrapolated. This provides a disciplined separation: disks are a 2D band regime where overlap changes the force law; clusters are a candidate 3D regime where overlap enhances gravitational strength within the standard scaling.

C.4 Lensing: Minimal Requirements and Qualitative Predictions

Gravitational lensing depends on the spacetime metric potentials (often denoted Φ and Ψ in weak-field cosmology), not only on the Newtonian acceleration inferred from rotation curves. In GR, the deflection is sensitive to the lensing potential $(\Phi + \Psi)/2$.

Implication. Any TPB overlap mechanism must be embedded in a covariant gravitational sector to predict lensing robustly. The main text flags this as future work (§6.3, Remark on covariant completion).

Nevertheless, the disk mechanism implies a robust qualitative signature: disk-driven overlap contributions should produce orientation-dependent lensing asymmetry aligned with the disk plane, unlike spherical CDM halos (see also §9.2 and §9.4.2). This can be tested statistically with galaxy–galaxy lensing: stacked lensing around disk galaxies binned by inclination should show measurable anisotropy if the overlap component is significant.

Intermediate falsifier. If lensing around disk galaxies is consistent with quasi-spherical halos with no inclination dependence beyond baryonic disk effects, then any disk-confined overlap contribution must be subdominant.

C.5 CMB Acoustic Peaks: What Any Replacement Must Reproduce

In ΛCDM, cold dark matter plays two key roles in the CMB: it deepens gravitational potential wells without coupling to photons (shifting peak heights and phases), and it supports early structure growth prior to recombination.

A TPB-only disk mechanism does not address this, because it is a late-time, galactic-scale ordering phenomenon. Therefore, a programme claiming full replacement must supply either: (a) an early-universe overlap sector — perhaps a cosmological-scale ordering of TPB commitment structure tied to the approximately homogeneous matter distribution at high redshift, before disk formation — that behaves effectively like a pressureless gravitational component at recombination, or (b) a modification of the gravitational response at early times (analogous in spirit to scalar-tensor extensions of GR) that reproduces equivalent potential evolution without particle dark matter. This appendix does not assert which route is correct; it identifies the requirement and notes that route (a) would represent a different ordering morphology of the same $a(\mathbf{x})$ framework, while route (b) would require a separate gravitational sector within VERSF.

C.6 Structure Formation: Growth Rate Constraint

Large-scale structure growth requires enhanced gravitational clustering in the matter-dominated era, consistency with observed $f\sigma_8(z)$, and consistency with the baryon acoustic oscillation (BAO) imprint.

A purely disk-confined late-time overlap mechanism cannot drive early structure formation. Therefore, if the TPB overlap programme aims to replace dark matter globally, it must include a second mechanism operating in the early universe or at cosmological scales.

C.7 Two-Mechanism Programme: Local Disk Regime + Cosmological Regime

A coherent way to unify the programme is to treat TPB overlap as admitting multiple ordered morphologies depending on $a(\mathbf{x})$:

- **Regime A** (Disk band ordering): thin $\Sigma \rightarrow$ 2D Poisson $\rightarrow$ logarithmic potential $\rightarrow$ flat rotation curves (this paper).
- **Regime B** (Cosmological / volumetric ordering): extended 3D ordering or filamentary ordering $\rightarrow$ different Green's function $\rightarrow$ candidate contributor to cluster and cosmological potentials.

The programme thus becomes: the sign structure and geometry of the ordering parameter $a(\mathbf{x})$ determines the morphology of overlap ordering, which determines the effective gravitational response. This "morphology-dependence" is a strong discriminator from CDM, which assumes a broadly universal halo phenomenology.

C.8 Observable Intermediate Targets

Even before a full CMB/structure solution is built, the programme yields intermediate targets:

1. **Inclination-dependent lensing anisotropy** around disk galaxies (as in C.4).
2. **Cluster morphology dependence:** if overlap ordering occurs in cluster cores, lensing should correlate more strongly with baryonic gas morphology than with galaxy distribution alone.
3. **Redshift evolution:** if overlap ordering is threshold-driven, the onset and strength of the effect should evolve with the cosmic star formation history and disk settling; this predicts a redshift trend in disk rotation-curve anomalies at fixed baryonic mass. The expected direction is that flat rotation curve signatures should be *weaker* at high redshift, because early disks are thicker and less settled — degrading the thin-band condition $h_{eff} \ll R$ on which the dimensional reduction depends. Higher gas fractions at early times would increase commitment density and partially compensate, but the geometric requirement (thin coherence band) is the dominant constraint. Quantitatively, the onset redshift for robust flat rotation curves should correlate with the epoch of disk settling.

Failure of these intermediate tests would constrain or rule out overlap as a dominant contributor.

C.9 What This Appendix Does Not Claim

This appendix does not claim that the TPB overlap mechanism presented here already explains the Bullet Cluster, the CMB acoustic spectrum, or linear structure growth. It identifies what additional ingredients are required and how those ingredients could be framed within the same ordering-parameter logic, without introducing new particles.

C.10 Summary

The disk-coherence mechanism established in this paper is a controlled, regime-specific account of flat rotation curves. Extending the TPB overlap programme to clusters and cosmology requires a separate analysis of overlap ordering morphologies in 3D and their covariant gravitational embedding. The cleanest near-term discriminators are lensing anisotropy and morphology dependence, which provide falsifiable stepping-stones toward broader claims.

VERSF Theoretical Physics Program